nature neuroscience

The acute light-induction of sleep is mediated by OPN4-based photoreception

Daniela Lupi[1,3], Henrik Oster[1–3], Stewart Thompson[1,2] & Russell G Foster[1]

Sleep is regulated by both homeostatic and circadian mechanisms. The latter, termed 'process c', helps synchronize sleep-wake patterns to the appropriate time of the day. However, in the absence of a circadian clock, overall sleep-wake rhythmicity is preserved and remains synchronized to the external light-dark cycle, indicating that there is an additional, clock-independent photic input to sleep. We found that the direct photic regulation of sleep in mice is predominantly mediated by melanopsin (OPN4)-based photoreception of photosensitive retinal ganglion cells (pRGCs). Moreover, OPN4-dependent sleep regulation was correlated with the activation of sleep-promoting neurons in the ventrolateral preoptic area and the superior colliculus. Collectively, our findings describe a previously unknown pathway in sleep regulation and identify the pRGC/OPN4 signaling system as a potentially new pharmacological target for the selective manipulation of sleep and arousal states.

The eyes collect and process light to generate an image of the world, but pattern detection is not their only function. Retinal photoreceptors also provide a measurement of environmental brightness (irradiance) that regulates nonvisual responses that range from pupil constriction to the entrainment of circadian rhythms[1]. The discovery that such irradiance responses persist in the absence of the rods and cones[2–4] paved the way for the identification of a subset of pRGCs that utilize the photopigment melanopsin[5–8]. It was originally assumed that OPN4 pRGCs and rods/cones form two functionally distinct and nonoverlapping pathways, with the rods and cones mediating image detection and the pRGCs handling irradiance-detection tasks. We now appreciate, however, that there is considerable overlap between the two systems. For example, both rods/cones and OPN4 contribute to the entrainment of the circadian timing system[8–10], and for pupil constriction the rods/cones provide the primary input at low irradiances, whereas full constriction under bright light requires functional OPN4 (refs. 4,11,12).

The regulation of sleep by light occurs via circadian clock–dependent and clock-independent pathways[13]. The light/dark cycle entrains the circadian timing system, which in turn acts to time sleep and arousal[14]. Independently, light also acutely modulates sleep. Although light promotes sleep in nocturnal animals, it increases alertness in diurnal species. In humans, for example, exposure to broad-spectrum white light at night has acute and dose-dependent effects on vigilance, reaction times, attentional failures and electroencephalogram (EEG) rhythms[15]. In rats, light exposure suppresses motor activity and enhances both rapid eye movement (REM) and non-REM sleep, whereas darkness promotes wakefulness[14,16,17]. Although such responses to light have been well documented in a range of species, little is known about the photoreceptors that mediate the direct effects of light on sleep.

We sought to address three related issues: the synchronization of sleep-wake rhythms by light, the acute modulation of sleep states by light and the relative contribution of rods, cones and pRGCs to these responses. We found that diurnal sleep-wake synchronization involves both rod/cone and melanopsin input. In contrast, we found that the acute induction of sleep by light is entirely dependent on melanopsin-based pRGC input and involves a direct activation of specific sleep-promoting centers of the brain, including the ventrolateral preoptic nuclei (VLPO) and the superior colliculus.

RESULTS

Diurnal entrainment of activity and sleep-wake rhythms

The synchronization of the sleep-wake cycle with external time is believed to be mediated via the regulation of the circadian timing system (process c)[18]. To assess the contribution of the different photoreceptive systems of the retina to this synchronization, we monitored wheel-running activity (as a readout of circadian pacemaker function) and EEG/electromyogram (EMG) potentials (to reflect sleep state) of mice lacking either rods and cones (*rd/rd cl*, carrying the *rd1* mutation in the *Pde6b* gene (*rd*) and expressing diphteria toxin under the control of the human *OPN1LW* promoter (*cl*)) or melanopsin ($Opn4^{-/-}$). Under standard 12-h light/12-h dark (L/D) conditions, wheel-running activity rhythms were indistinguishable between *rd/rd cl* animals and congenic C3H wild-type controls (**Fig. 1a** and **Table 1**). These data confirm previous findings that indicate that visual photoreceptors are dispensable for the normal entrainment of

[1]Circadian and Visual Neuroscience Group, Nuffield Laboratory of Ophthalmology, Levels 5 and 6 West Wing, John Radcliffe Hospital, Headley Way, Headington, Oxford OX3 9DU, UK. [2]Present addresses: Circadian Rhythms Group, Max Planck Institute for Biophysical Chemistry, Am Fassberg 11, 37077 Göttingen, Germany (H.O.) and Howard Hughes Medical Institute, Department of Ophthalmology and Visual Sciences, University of Iowa, Iowa City, Iowa 52242, USA (S.T.). [3]These authors contributed equally to this work. Correspondence should be addressed to R.G.F. (russell.foster@eye.ox.ac.uk).

Received 9 April; accepted 1 July; published online 17 August 2008; doi:10.1038/nn.2179

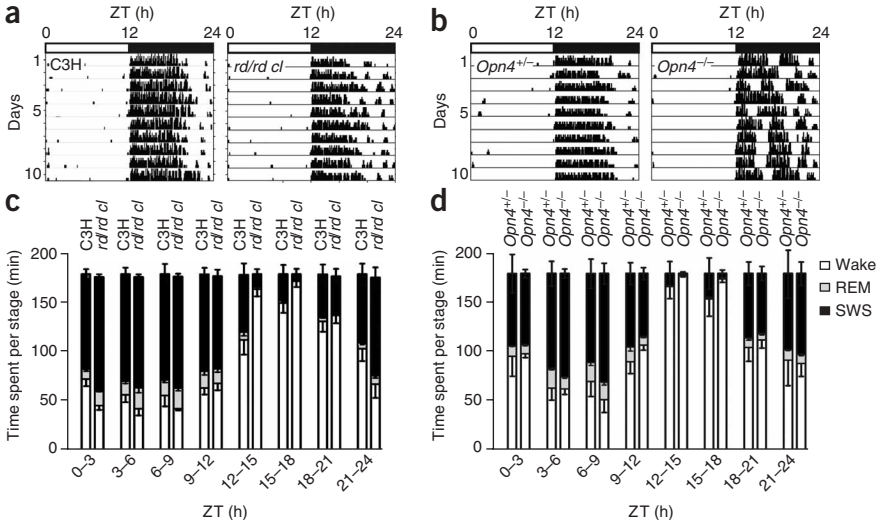

Figure 1 Rods/cones alone or pRGCs alone are sufficient to entrain the circadian clock and sleep-wake rhythms. (**a**,**b**) Representative wheel-running recordings (actograms) of C3H (**a**, left), *rd/rd cl* (**a**, right), *Opn4*$^{+/-}$ (**b**, left) and *Opn4*$^{-/-}$ mice (**b**, right). Vertical black bars represent running-wheel activity. Consecutive days are plotted beneath each other. Horizontal bars on top indicate the L/D regimen. (**c**,**d**) Diurnal sleep/wake profiles of wild-type (C3H), rodless/coneless (*rd/rd cl*) (**c**), *Opn4*$^{+/-}$ and *Opn4*$^{-/-}$ mice (**d**) were assessed by EEG/EMG recordings under L/D conditions. Data were analyzed in 3-h bins starting at 'lights on' (ZT 0). No significant differences were detected between the different genotypes ($P > 0.05$ for all comparisons, two-way ANOVA with the variables 'time' and 'genotype' followed by Bonferroni post test for all three sleep-wake stages; see also **Supplementary Table 1**). All data shown are averages ± s.e.m. ($n = 4$).

the circadian timing system[2,19–21]. Similarly, light entrainment of wheel-running activity was largely unaffected in mice lacking functional pRGC photoreception (*Opn4*$^{-/-}$). *Opn4*$^{-/-}$ mice showed very similar activity profiles when compared to *Opn4*$^{+/-}$ littermate controls (**Fig. 1b**). Notably, closer inspection revealed that the activity onsets were less precise in mice lacking *Opn4* (**Table 1**), which supports earlier reports of decreased, but largely sufficient, light sensitivity of the circadian clock in *Opn4*$^{-/-}$ mice[9,10].

We then monitored sleep-wake patterns and sleep macro architecture by combined EEG/EMG recordings using implanted radio transmitters in freely moving mice. As we observed for wheel-running activity, the entrainment of sleep-wake rhythms in *rd/rd cl* animals was indistinguishable from that of fully sighted mice (**Fig. 1c** and **Supplementary Table 1** online), suggesting again that OPN4 can fully compensate for rod/cone loss under standard L/D conditions. Likewise, sleep-wake–cycle entrainment was not affected by *Opn4*-deficiency. *Opn4*$^{-/-}$ mice had normal sleep-wake patterns and sleep phase distribution under L/D conditions (**Fig. 1d** and **Supplementary Table 1**). Collectively, these results demonstrate that a mixed rod/cone and OPN4 input accounts for both wheel-running activity and sleep-wake–cycle entrainment. Either the rods/cones alone or pRGCs alone can provide irradiance information to synchronize these internal rhythms with external time[8–10].

Melanopsin mediates photic sleep induction

Because diurnal entrainment of the sleep-wake cycle is, at least in part, regulated by process c[18] and the circadian clock has been shown to be regulated by both rods/cones and melanopsin-based pRGC input[8], we then explored the contribution of both systems in the clock-independent regulation of sleep-wake states by light (see above). We examined sleep induction in *rd/rd cl* and *Opn4*$^{-/-}$ mice by exposing them to a 1-h light pulse starting 4 h after 'lights off' (Zeitgeber time (ZT) 16) (**Fig. 2**). In wild-type mice, white light of 200 μW cm^{-2} induced sleep in 5–8 min, as defined by simultaneous power spectrum analysis of the EEG and EMG amplitude monitoring (**Fig. 2a**). This effect was preserved in *rd/rd cl* mice (**Fig. 2a**). Moreover, the distribution of different sleep-wake states throughout the 60-min light exposure was comparable for both genotypes (**Fig. 2c–e**). The time spent awake was reduced by 60-70% in both wild-type and *rd/rd cl* mice (**Fig. 2c**), whereas both REM and slow-wave sleep (SWS) were correspondingly increased in both genotypes (**Fig. 2d**,**e**).

Previous experiments have shown that irradiance responses, such as the pupillary light reflex, depend on the input of both rods/cones and OPN4 in an intensity-dependent manner, with rods/cones acting at low irradiances and melanopsin acting at higher light levels[4,11]. We therefore determined the full irradiance response curves for sleep induction in both wild-type and *rd/rd cl* mice. The effect of light intensity on the amount of SWS and REM sleep for the two genotypes was indistinguishable, with both showing saturating responses between 50–100 μW cm^{-2} (**Supplementary Fig. 1** online). Notably, sleep latency (defined as the time between the beginning of the light exposure and the first 10-s sleep bout) was very similar at all irradiances tested, both within and between genotypes (**Supplementary Fig. 1**). This strongly suggests that any increase in total sleep duration that we observed at higher irradiances results from a longer lasting, rather than a quicker acting, induction of sleep by light.

Photic sleep induction has also been correlated with the activation of sleep-promoting neurons in the VLPO[22,23]. We therefore tested VLPO activation in the absence of rods and cones by immunohistochemical detection of FOS protein after nocturnal light exposure. In both wild-type and *rd/rd cl* mice, light strongly increased FOS protein levels in this area, with no significant differences being observed between both genotypes ($P = 0.7$; **Supplementary Fig. 2** online). These data, along with our behavioral analysis, indicate that rods and cones are dispensable for the direct photic modulation of sleep.

To asses the role of melanopsin photoreception in the acute effects of light on sleep, *Opn4*$^{-/-}$ [11] and control *Opn4*$^{+/-}$ mice were used in the same experimental procedure that we used for the *rd/rd cl* mice. Although sleep-wake phase and distribution were unaltered in *Opn4*$^{-/-}$ mice (**Fig. 1d**), light-mediated sleep induction was found to be markedly affected. Control animals readily showed sleep induction

Table 1 Entrainment parameters of wheel-running activity of rod/cone- and *Opn4*-deficient mice

Genotype	Onset time (ZT)	Onset variation (min)	α phase (h)
C3H	12.03 ± 0.02	3.4 ± 0.6	12.4 ± 0.3
rd/rd cl	12.02 ± 0.03	3.8 ± 1.2	12.3 ± 0.1
Opn4$^{+/-}$	12.15 ± 0.02	3.6 ± 0.6	11.4 ± 0.1
Opn4$^{-/-}$	12.18 ± 0.04	6.0 ± 0.8*	11.5 ± 0.3

*$P < 0.05$ (two-tailed Mann-Whitney test); $n = 10$ for all genotypes.

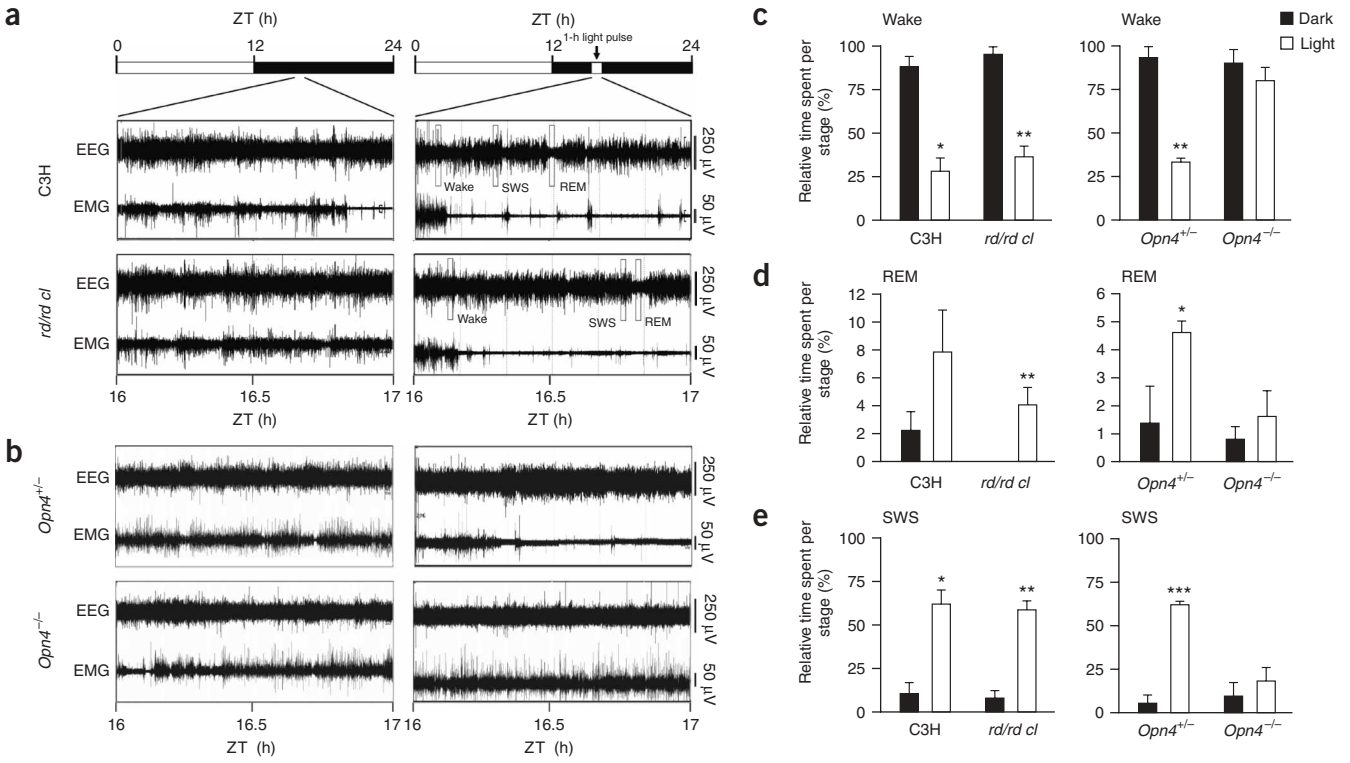

Figure 2 OPN4, but not rods and cones, regulates the acute light-induced sleep response in mice. (**a**,**b**) Representative EEG and EMG traces of wild-type (**a**, upper), *rd/rd cl* (**a**, lower), *Opn4*$^{+/-}$ (**b**, upper) and *Opn4*$^{-/-}$ (**b**, lower) mice at ZT16–17 without (left) and with (right) light exposure at 200 μW cm^{-2}. Light schedules are depicted by black and white bars above the panels. Representative wake, SWS and REM episodes are depicted by black boxes in the EEG traces of C3H and *rd/rd cl* mice. (**c**–**e**) Quantification of photic effects on different sleep-wake stages at ZT16–17. All data are averages ± s.e.m. ($n = 4$; $^{*}P < 0.05$, $^{**}P < 0.01$, two-tailed Wilcoxon rank sum test).

on light exposure at ZT16 (**Fig. 2b**). Light-induced wake suppression (**Fig. 2c**), REM (**Fig. 2d**) and SWS induction (**Fig. 2e**) were largely comparable to the results obtained in both wild-type and *rd/rd cl* mice. However, *Opn4*$^{-/-}$ mice failed entirely to respond to light, even at very bright irradiances (>200 μW cm^{-2}; **Fig. 2b**). This complete lack of sleep modulation by even very bright light suggests that the pRGC photoreceptive system provides the exclusive pathway for mediating the acute effects of light on sleep.

Masking and sleep induction use non-identical pathways

It has been reported previously that negative masking, that is, the (clock independent) suppression of locomotor activity by high illumination levels, is attenuated by the deletion of *Opn4* in mice[24]. Similarly, our results indicate that masking behavior is also attenuated in *Opn4*$^{-/-}$ mice. To evaluate the extent to which masking and photic sleep modulation mechanisms overlap, we compared wheel-running activity and sleep responses in our mice. Under normal L/D conditions, both C3H and *rd/rd cl* mice showed continuous and robust wheel-running behavior during the second quarter of the night (**Fig. 3a**). When the lights were switched on at ZT16, animals of both genotypes rapidly and uniformly ceased wheel-running and only resumed activity after the lights had been switched off again (ZT17) (**Fig. 3a**).

In the same manner, *Opn4*$^{-/-}$ and *Opn4*$^{+/-}$ animals showed robust wheel-running activity between ZT15 and ZT18 under L/D conditions (**Fig. 3b**). When the lights were switched on at ZT16, *Opn4*$^{+/-}$ animals rapidly stopped using the wheel for the whole time of light exposure, whereas the suppression of running-wheel activity was incomplete in *Opn4*$^{-/-}$ mice (**Fig. 3b**). The suppression levels were 95% (*Opn4*$^{+/-}$) versus 58% (*Opn4*$^{-/-}$). In comparison, locomotor activity was reduced by 97% in C3H and 95% in *rd/rd cl* mice, respectively (**Fig. 3c**). Thus, negative masking, although at a decreased efficiency, was preserved in the absence of OPN4, whereas sleep induction was completely abolished (**Fig. 3d**). These data confirm previous reports that masking utilizes both the rod/cone and pRGC photoreceptive systems[24] and demonstrate for the first time that sleep induction relies either predominantly or exclusively on OPN4/pRGC photoreception.

OPN4-mediated activation of brain sleep-wake centers

OPN4-based pRGCs have been shown to send monosynaptic projections to various brain regions including sleep-promoting centers in the basal forebrain and the hindbrain[25]. To assess whether some of these structures might be the anatomical targets by which pRGC photoreceptors interact with the sleep-wake regulatory system, we compared neuronal activation of the VLPO, superior colliculus and SCN in response to nocturnal light exposure in *Opn4*$^{-/-}$ and *Opn4*$^{+/-}$ mice by quantifying *Fos* mRNA expression levels using quantitative PCR (qPCR). In the rodent brain, the VLPO is characterized by a marked expression of the neurotransmitter Galanin (*Gal*)[26]. We used *Gal* mRNA *in situ* hybridization to define the VLPO in brain sections from wild-type and *Opn4*$^{-/-}$ mice (**Fig. 4a**,**b**).

Total RNA extracts were prepared from tissue punches from the liver, the SCN, the VLPO (**Supplementary Fig. 3** online) and the superior colliculus. The correct targeting of punches was confirmed by standard reverse transcription–PCR (RT-PCR) using site-specific marker genes (*Six6* for the SCN[27], *Gal* for the VLPO[26] and *Pax7* for the superior colliculus[28]) with *Ef1α* as a positive control (**Fig. 4c**). As described

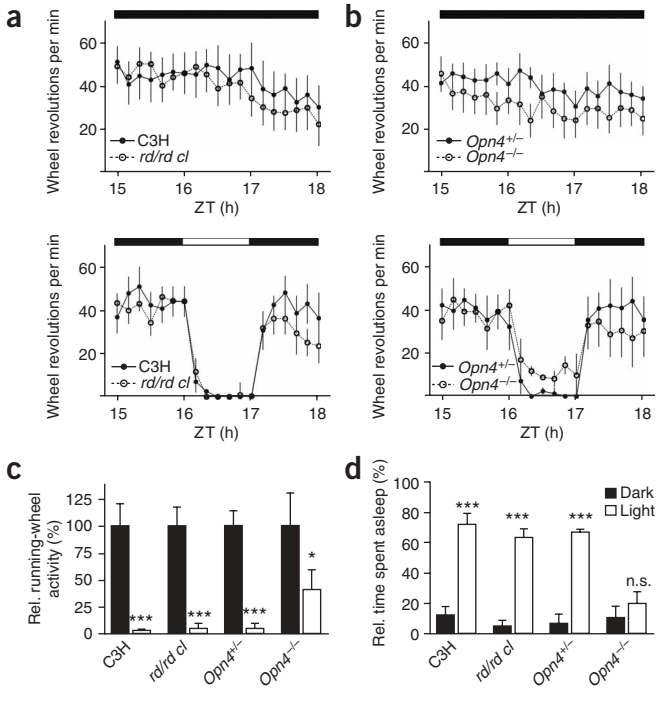

Figure 3 Masking responses to light are preserved in *Opn4*$^{-/-}$ mice. (**a**,**b**) Wheel-running activities of C3H and *rd/rd cl* (**a**), *Opn4*$^{+/-}$ and *Opn4*$^{-/-}$ (**b**) mice between ZT15 and ZT18 under normal L/D conditions (upper) and in response to 1 h of nocturnal light exposure starting at ZT16 (lower). Horizontal bars depict lighting conditions. (**c**) Quantification of the level of masking activity in responses to light exposure at ZT16 in the different genotypes. Black bars represent dark controls and white bars depict light-pulsed animals. (**d**) Quantification of total sleep induction in response to light exposure at ZT16 in the different genotypes. Black bars represent dark controls and white bars depict light-pulsed animals. All data are averages ± s.e.m. ($n = 10$ for wheel running and 4 for sleep data; $^{*}P < 0.05$, $^{**}P < 0.01$, $^{***}P < 0.001$, two-tailed Mann-Whitney rank sum test).

previously[10], photic induction of *Fos* in the SCN was attenuated, but not absent, in *Opn4*$^{-/-}$ mice (**Fig. 4d**). Notably, *Fos* activation in the VLPO (**Fig. 4e**) and in the superior colliculus (**Fig. 4f**) was completely abolished in the absence of *Opn4*. In the VLPO, these findings were confirmed by normalizing *Fos* expression to the amount of *Gal* transcript that was present in the tissue punches (**Supplementary Fig. 4** online). The absence of *Fos* induction in sleep-regulatory centers, together with the abolished sleep response to light in *Opn4*$^{-/-}$ mice, strongly suggests that pRGC-originating direct activation of these target sites forms the basis of the observed clock-independent sleep regulation by light.

DISCUSSION

Our data provide strong evidence for a predominantly, perhaps exclusively, OPN4-mediated photic input into the sleep-wake regulatory system that involves activation of neurons in the VLPO and/or the superior colliculus. The finding that rods and cones have no apparent role in light-induced sleep was not expected and distinguishes this process from all other irradiance-dependent responses described thus far. This finding is all the more notable in view of a recent study showing that the pRGCs provide the route by which OPN4 and the rods/cones reach many brain nuclei[29], raising the question of how OPN4 and rod/cone inputs are functionally separated at the level of the pRGCs.

As mentioned above, circadian entrainment, pupil constriction and masking all arise from a mixed rod/cone and OPN4 input[3,4,8,11,24]. It remains unclear what sensory information the different photoreceptors (rods, cones and OPN4) provide to these processes, but their input may be related to both the latency and dynamic range of the response in question. It seems probable that the rods/cones mediate short latency and dim-light detection, whereas OPN4 controls longer latency and bright-light responses[30]. This hypothesis is consistent with the results presented here, which show that sleep is induced after 7–10 min and at irradiances greater than 50 μW cm^{-2}. Although a direct comparison is complex, the irradiances needed for sleep induction are far greater than the threshold response for pupil constriction (for example, full constriction occurs in seconds with less than 0.5 μW cm^{-2})[12], circadian phase shifting[2] or melatonin suppression (15-min light stimulus at 0.001 μW cm^{-2})[3]. We suggest, therefore, that the apparent absence of a rod/cone input to the acute regulation of sleep relates to the fact that this is a long latency and bright-light response. At this point we cannot entirely exclude that some residual sleep induction might occur in *Opn4*$^{-/-}$ mice at even higher illumination levels (>200 μW cm^{-2})

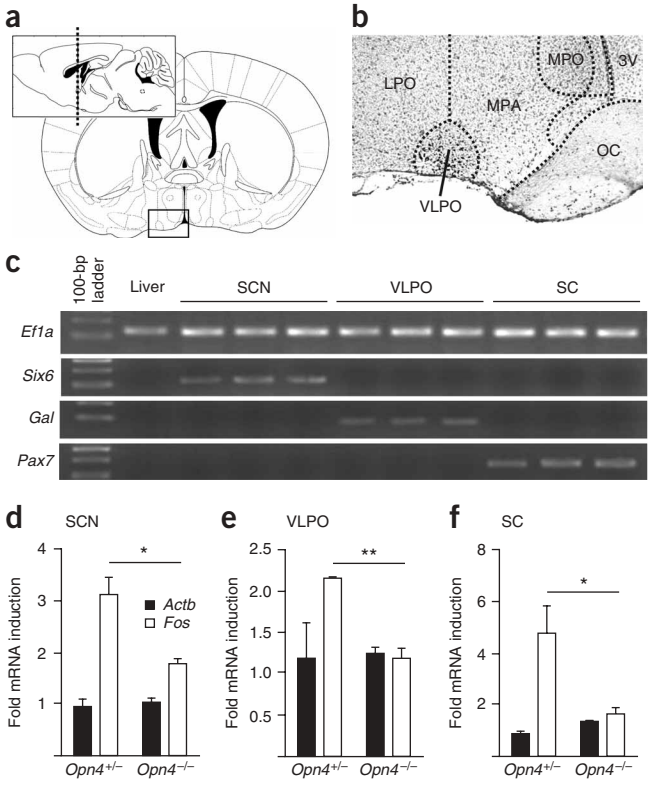

Figure 4 Light-induced *Fos* transcription is abolished in the VLPO and superior colliculus of *Opn4*$^{-/-}$. (**a**) Diagram illustrating the localization of the VLPO in the adult mouse brain (modified from ref. 47). (**b**) *Gal in situ* hybridization in the preoptic area. The ventral preoptic area shown corresponds to the area depicted by the rectangle in **a**. The VLPO borders are marked by dotted lines (3V, third ventricle; LPO, lateral preoptic nucleus; MPA, medial preoptic area; MPO, medial preoptic nucleus; OC, optic chiasm). (**c**) RT-PCR was used to assess tissue punch accuracy. One liver punch and three punches each for SCN, VLPO and superior colliculus (SC) are shown. (**d**–**f**) *Actb* and *Fos* mRNA induction in the SCN (**d**), the VLPO (**e**) and the superior colliculus (**f**) after 1 h of nocturnal light exposure in *Opn4*$^{+/-}$ and *Opn4*$^{-/-}$ animals (all data are averages ± s.e.m. ($n = 3$); $^{*}P < 0.05$, $^{**}P < 0.01$, two-tailed Mann-Whitney test).

based on an input from rods/cones. This seem unlikely, however, as any rod/cone input would be several log units less effective than OPN4 photoreception and, as a result, would contribute very little to the response under natural conditions. Furthermore, rods/cones typically mediate low-level, rather than very bright, irradiance responses to light.

Recently, pRGCs have been shown to send monosynaptic projections to the sleep-promoting centers of the basal forebrain[25]. This suggests that light can induce sleep directly via pRGC-mediated activation of these structures. Our findings relating to the photic activation of VLPO neurons would support this view. Such acute activation of sleep-promoting brain nuclei might explain how circadian clock–deficient mice can still show a 24-h activity rhythm under an L/D cycle[31–35]. Furthermore, impaired masking behavior and even inverted daily activity profiles have been observed in *Opn4*$^{-/-}$ mice (**Fig. 3**)[24,36], providing additional support for a direct input of the pRGCs in sleep and arousal control. The superior colliculus has also been strongly implicated in the photic regulation of sleep[37] and receives a direct input from OPN4-based pRGCs[22,25]. Here we show that *Opn4*$^{-/-}$ mice lack any *Fos* induction in this region. We found this to be a particularly surprising result in view of the major retinal projection to the superior colliculus that originates from the rods and cones[38], and it suggests that pRGC photoreception may be more important in superior colliculus function than previously envisaged. Collectively, our results indicate that light does not act exclusively through one brain region (for example, the VLPO), but that parallel signals via the superior colliculus, and probably other retino-recipient areas, reach the arousal system and inhibit wake-promoting neurons.

Currently, there are no studies that provide a direct link between the alerting effects of light and the pRGCs in humans, but some strong suggestive evidence has emerged recently. The alerting effect of light has been studied in human subjects by comparing green (~555 nm) and blue (~460 nm) light. Blue light was shown to be consistently more effective at increasing levels of alertness and decreasing sleepiness[15]. The spectral response of melanopsin has been shown to peak at 480 nm in mice[4], nonhuman primates[39] and human subjects[40]. In contrast, the human photopic visual sensitivity peaks near 555 nm. These data provide compelling supportive evidence that humans, like mice, use their pRGCs to provide the photoreceptive input for the acute regulation of sleep. Should this be the case, then the melanopsin phototransduction signaling cascade[12] could provide a powerful new therapeutic target for the direct pharmacological manipulation of sleep and arousal states in humans.

METHODS

Animals. All aspects of animal work were carried out under license and in accordance with the Animal (Scientific Procedures) Act 1986, UK. We used 4–6-month-old male mice for all assays. *rd/rd cl* mice were kept on a C3H genetic background, and age-matched C3H wild-type mice, which were not carrying the *rd* mutation, were used as controls. *Opn4*$^{-/-}$ mice[11] were maintained on a C57Bl/6 × 129Sv background as heterozygous breeders. *Opn4*$^{-/-}$ offspring and heterozygous littermates were used for all experiments.

Wheel running–activity monitoring. We assessed locomotor activity by wheel-running monitoring as described previously[41,42]. Briefly, mice were placed in running-wheel cages under an L/D cycle for 2 weeks before the experiment. For L/D analyses, mice were kept in L/D for an additional 10 d and entrainment, activity onset and activity phases were determined using the ClockLab software package (Actimetrics). Onset variation was calculated by fitting a regression line through ten consecutive onsets and measuring the deviation of actual onsets from that line. For masking responses, lights (white fluorescent lights, 200 μW cm^{-2}) were switched on for 1 h at ZT16 and wheel revolutions were compared with those of the same time interval on the preceding day for each animal.

Sleep recordings. EEG and EMG recordings from adult male mice carrying subcutaneously implanted telemetry transmitters (Model F20-EET, DSI) for simultaneous recording of two biopotentials (EEG and EMG) were collected for 48 h per experiment. During the first 24 h, we obtained diurnal sleep-wake rhythms and baseline dark control traces at 4–5 h after 'lights off' (ZT16–17). On the second day, light pulses of different irradiances (50–400 μW cm^{-2}) were given using a halogen light source and optical fiber guides and starting at ZT16 to assess acute photic sleep modulation. Biopotential data were analyzed using the SleepSign software package (Kissei-Comtec) at 10-s intervals. All automatic scoring results were independently confirmed using manual blind scoring by experienced researchers.

Immunohistochemistry. FOS immunostaining on frozen sections with or without prior light exposure was carried out as described previously[43]. Briefly, peroxide-blocked sections were incubated with FOS antibody (1:1,000, Oncogene) at 4 °C overnight, followed by avidin/biotin amplification and peroxidase/3,3′-diaminobenzidine detection (Vectastain Elite kit, Vector Labs).

***In situ* hybridization.** mRNA labeling for *Gal* on frozen sections was carried out as described previously[44]. Briefly, 20-μm frozen sections were mounted on slides, post-fixed, acetylated and hybridized with digoxinenin-labeled RNA probes overnight at 58 °C. We carried out antigenic detection using peroxidase-coupled antibodies followed by tyramide amplification and biotin-coupled alkaline phosphatase/5-bromo-4-chloro-3′-indolyphosphate p-toluidine salt/nitro-blue tetrazolium chloride detection. We used 5′-ACC GAG AGA GCC TTG ATC CT-3′ and 5′-CAG AGG ATT GGC TTG AGG AG-3′ as forward and reverse primers to amplify the *Gal* template from whole mouse-brain cDNA samples.

RT-PCR and quantitative PCR. Reverse-transcribed total RNA preparations (RNeasy Micro Kit, Qiagen) from 1-mm tissue punches were PCR-amplified using an Eppendorf Mastercycler for RT-PCR or a StepOne Realtime PCR system (Applied Biosystems) and SYBR Green detection for qPCR. Cycling conditions were 3 min at 94 °C and 30 (RT-PCR) or 40 (qPCR) cycles of 30 s at 94 °C, 30 s at 60 °C and 30 s at 72 °C for 30, followed by 5 min at 72 °C. We used the following primers: 5′-AGA GAA ACG GAG AAT CCG AAG GGA-3′ and 5′-ATT GGC AAT CTC AGT CTG CAA CGC-3′ for *Fos*, 5′-CAA CAC TGT TTG CTG CCT GTG GAT-3′ and 5′-ACT CTT AGG ATG GGT GGC AGA AGT-3′ for *Ef1α*, 5′-AGA GTG GTA CCT TCA GGA CCC ATA-3′ and 5′-AGA ACC TGC TGC TGG AGT CTG TTT-3′ for *Six6*, 5′-ATG CCT GCA AAG GAG AAG AGA GGT-3′ and 5′-TCT GTG GTT GTC AAT GGC ATG TGG-3′ for *Gal*, 5′-GCG AGA AGA AAG CCA AAC ACA GCA-3′ and 5′-ATT CCA CAT CTG AGC CCT CAT CCA-3′ for *Pax7*, and 5′-CAG CTT CTT TGC AGC TCC TTC GTT-3′ and 5′-TTC TGA CCC ATT CCC ACC ATC ACA-3′ for *Actb*. Relative quantification of transcript levels was carried out as described previously[45,46].

Statistical analysis. For comparisons between and within two groups, we used two-tailed Mann-Whitney (unpaired) or Wilcoxon (paired) rank sum tests, reflecting the small sample sizes (n = 4–10) for which Gaussian distribution could not be automatically assumed. All datasets with multiple comparisons were analyzed by two-way ANOVA followed by Bonferroni post-test. $P < 0.05$ was considered to be statistically significant. Analyses were carried out using Microsoft Excel or GraphPad Prism software. All data are presented as means ± s.e.m.

Note: Supplementary information is available on the Nature Neuroscience website.

ACKNOWLEDGMENTS

We thank S. Hattar (Johns Hopkins University) for generously donating the *Opn4*$^{-/-}$ mice, N. Naujokat for technical assistance and S.N. Peirson for helpful comments on this manuscript. This work was supported by a Wellcome Trust Program grant and a European Commission grant (EuClock) to R.G.F. H.O. was supported by an Otto Hahn fellowship of the Max Planck Society and an Emmy Noether fellowship of the Deutsche Forschungsgemeinschaft.

AUTHOR CONTRIBUTIONS

R.G.F. conceived the project. D.L. conducted the sleep and immunohistochemical analyses. H.O. undertook the wheel running, the *in situ* and the qPCR analyses.

S.T. set up and contributed to the sleep experiments. R.G.F., H.O. and D.L. wrote the paper, with advice from S.T.

Published online at http://www.nature.com/natureneuroscience/
Reprints and permissions information is available online at http://npg.nature.com/reprintsandpermissions/

1. Foster, R.G. *et al.* Non-rod, non-cone photoreception in rodents and teleost fish. *Novartis Found. Symp.* **253**, 3–23; discussion 23–30, 52–55, 102–109 (2003).
2. Freedman, M.S. *et al.* Regulation of mammalian circadian behavior by non-rod, non-cone, ocular photoreceptors. *Science* **284**, 502–504 (1999).
3. Lucas, R.J., Freedman, M.S., Munoz, M., Garcia-Fernandez, J.M. & Foster, R.G. Regulation of the mammalian pineal by non-rod, non-cone, ocular photoreceptors. *Science* **284**, 505–507 (1999).
4. Lucas, R.J., Douglas, R.H. & Foster, R.G. Characterization of an ocular photopigment capable of driving pupillary constriction in mice. *Nat. Neurosci.* **4**, 621–626 (2001).
5. Provencio, I., Rollag, M.D. & Castrucci, A.M. Photoreceptive net in the mammalian retina. This mesh of cells may explain how some blind mice can still tell day from night. *Nature* **415**, 493 (2002).
6. Berson, D.M., Dunn, F.A. & Takao, M. Phototransduction by retinal ganglion cells that set the circadian clock. *Science* **295**, 1070–1073 (2002).
7. Sekaran, S., Foster, R.G., Lucas, R.J. & Hankins, M.W. Calcium imaging reveals a network of intrinsically light-sensitive inner-retinal neurons. *Curr. Biol.* **13**, 1290–1298 (2003).
8. Hattar, S. *et al.* Melanopsin and rod-cone photoreceptive systems account for all major accessory visual functions in mice. *Nature* **424**, 75–81 (2003).
9. Panda, S. *et al.* Melanopsin (Opn4) requirement for normal light-induced circadian phase shifting. *Science* **298**, 2213–2216 (2002).
10. Ruby, N.F. *et al.* Role of melanopsin in circadian responses to light. *Science* **298**, 2211–2213 (2002).
11. Lucas, R.J. *et al.* Diminished pupillary light reflex at high irradiances in melanopsin-knockout mice. *Science* **299**, 245–247 (2003).
12. Peirson, S.N. *et al.* Microarray analysis and functional genomics identify novel components of melanopsin signaling. *Curr. Biol.* **17**, 1363–1372 (2007).
13. Borbely, A.A. Effects of light on sleep and activity rhythms. *Prog. Neurobiol.* **10**, 1–31 (1978).
14. Saper, C.B., Scammell, T.E. & Lu, J. Hypothalamic regulation of sleep and circadian rhythms. *Nature* **437**, 1257–1263 (2005).
15. Lockley, S.W. *et al.* Short-wavelength sensitivity for the direct effects of light on alertness, vigilance and the waking electroencephalogram in humans. *Sleep* **29**, 161–168 (2006).
16. Benca, R.M., Gilliland, M.A. & Obermeyer, W.H. Effects of lighting conditions on sleep and wakefulness in albino Lewis and pigmented Brown Norway rats. *Sleep* **21**, 451–460 (1998).
17. Borbely, A.A. Sleep and motor activity of the rat during ultra-short light-dark cycles. *Brain Res.* **114**, 305–317 (1976).
18. Borbely, A.A. A two process model of sleep regulation. *Hum. Neurobiol.* **1**, 195–204 (1982).
19. David-Gray, Z.K., Janssen, J.W., DeGrip, W.J., Nevo, E. & Foster, R.G. Light detection in a 'blind' mammal. *Nat. Neurosci.* **1**, 655–656 (1998).
20. Provencio, I., Wong, S., Lederman, A.B., Argamaso, S.M. & Foster, R.G. Visual and circadian responses to light in aged retinally degenerate mice. *Vision Res.* **34**, 1799–1806 (1994).
21. Foster, R.G. *et al.* Circadian photoreception in the retinally degenerate mouse (*rd/rd*). *J. Comp. Physiol. [A]* **169**, 39–50 (1991).
22. Gooley, J.J., Lu, J., Fischer, D. & Saper, C.B. A broad role for melanopsin in nonvisual photoreception. *J. Neurosci.* **23**, 7093–7106 (2003).
23. Fuller, P.M., Gooley, J.J. & Saper, C.B. Neurobiology of the sleep-wake cycle: sleep architecture, circadian regulation and regulatory feedback. *J. Biol. Rhythms* **21**, 482–493 (2006).
24. Mrosovsky, N. & Hattar, S. Impaired masking responses to light in melanopsin-knockout mice. *Chronobiol. Int.* **20**, 989–999 (2003).
25. Hattar, S. *et al.* Central projections of melanopsin-expressing retinal ganglion cells in the mouse. *J. Comp. Neurol.* **497**, 326–349 (2006).
26. Gaus, S.E., Strecker, R.E., Tate, B.A., Parker, R.A. & Saper, C.B. Ventrolateral preoptic nucleus contains sleep-active, galaninergic neurons in multiple mammalian species. *Neuroscience* **115**, 285–294 (2002).
27. Conte, I., Morcillo, J. & Bovolenta, P. Comparative analysis of Six3 and Six6 distribution in the developing and adult mouse brain. *Dev. Dyn.* **234**, 718–725 (2005).
28. Stoykova, A. & Gruss, P. Roles of *Pax* genes in developing and adult brain as suggested by expression patterns. *J. Neurosci.* **14**, 1395–1412 (1994).
29. Guler, A.D. *et al.* Melanopsin cells are the principal conduits for rod-cone input to non–image-forming vision. *Nature* **453**, 102–105 (2008).
30. Peirson, S. & Foster, R.G. Melanopsin: another way of signaling light. *Neuron* **49**, 331–339 (2006).
31. Bae, K., Lee, C., Hardin, P.E. & Edery, I. dCLOCK is present in limiting amounts and likely mediates daily interactions between the dCLOCK-CYC transcription factor and the PER-TIM complex. *J. Neurosci.* **20**, 1746–1753 (2000).
32. Kume, K. *et al.* mCRY1 and mCRY2 are essential components of the negative limb of the circadian clock feedback loop. *Cell* **98**, 193–205 (1999).
33. van der Horst, G.T. *et al.* Mammalian Cry1 and Cry2 are essential for maintenance of circadian rhythms. *Nature* **398**, 627–630 (1999).
34. Zheng, B. *et al.* Nonredundant roles of the *mPer1* and *mPer2* genes in the mammalian circadian clock. *Cell* **105**, 683–694 (2001).
35. Bunger, M.K. *et al.* Mop3 is an essential component of the master circadian pacemaker in mammals. *Cell* **103**, 1009–1017 (2000).
36. Mrosovsky, N. & Hattar, S. Diurnal mice (*Mus musculus*) and other examples of temporal niche switching. *J. Comp. Physiol. A Neuroethol. Sens. Neural Behav. Physiol.* **191**, 1011–1024 (2005).
37. Miller, A.M., Obermeyer, W.H., Behan, M. & Benca, R.M. The superior colliculus pretectum mediates the direct effects of light on sleep. *Proc. Natl. Acad. Sci. USA* **95**, 8957–8962 (1998).
38. Holt, C.E. & Harris, W.A. Position, guidance and mapping in the developing visual system. *J. Neurobiol.* **24**, 1400–1422 (1993).
39. Dacey, D.M. *et al.* Melanopsin-expressing ganglion cells in primate retina signal color and irradiance and project to the LGN. *Nature* **433**, 749–754 (2005).
40. Hankins, M.W. & Lucas, R.J. The primary visual pathway in humans is regulated according to long-term light exposure through the action of a nonclassical photopigment. *Curr. Biol.* **12**, 191–198 (2002).
41. Albrecht, U. & Foster, R.G. Placing ocular mutants into a functional context: a chronobiological approach. *Methods* **28**, 465–477 (2002).
42. Jud, C., Schmutz, I., Hampp, G., Oster, H. & Albrecht, U. A guideline for analyzing circadian wheel-running behavior in rodents under different lighting conditions. *Biol. Proced. Online* **7**, 101–116 (2005).
43. Rieux, C. *et al.* Analysis of immunohistochemical label of Fos protein in the suprachiasmatic nucleus: comparison of different methods of quantification. *J. Biol. Rhythms* **17**, 121–136 (2002).
44. Abraham, D., Oster, H., Huber, M. & Leitges, M. The expression pattern of three mast cell–specific proteases during mouse development. *Mol. Immunol.* **44**, 732–740 (2007).
45. Peirson, S.N., Butler, J.N. & Foster, R.G. Experimental validation of novel and conventional approaches to quantitative real-time PCR data analysis. *Nucleic Acids Res.* **31**, e73 (2003).
46. Oster, H. *et al.* The circadian rhythm of glucocorticoids is regulated by a gating mechanism residing in the adrenal cortical clock. *Cell Metab.* **4**, 163–173 (2006).
47. Paxinos, G. *et al. In vitro* autoradiographic localization of calcitonin and amylin binding sites in monkey brain. *J. Chem. Neuroanat.* **27**, 217–236 (2004).